 CMC, vol.6, no.1, pp.43-50, 2007

# Evaluations of the BGA Solder Ball Shape by Using Energy Method

**Heng Cheng Lin[1,2], Chieh Kung[3], Rong Sheng Chen[2]**

**Abstract:** Presented herein are the evaluation results of the BGA solder ball shape using energy method, two types of solder, viz. Sn37Pb and Sn80Pb, are selected .The geometry of the solder bump is firstly estimated using free computer software, the Surface Evolver, an interactive program which is an energy-based approach for the study of liquid droplet surfaces shaped by surface tension and other energies. The solder bump is then numerically constructed in a finite element model that simulates a BGA package. The influences of both upper and bottom solder pad radii, the surface tension on the balls, and the external load axially applied to the reflow solders on the stand-off height and the contact angle for both solder materials are investigated. The results show that for both solder materials, the stand-off height remains at a height under some pad radius. The height decreases as both upper and bottom pad radii increase. On the other hand, the contact angle presents a nearly inverse trend with respect to the pad radii. The study of the effect of surface tension reveals that at a constant pad radius, the solder ball stand-off height increases with surface tension; however, the trend becomes saturated eventually. The contact angle decreases as the surface tension becomes large. The trend also tends to be saturated. The results of the effects of axially applied load on the stand-off height and the contact angle show that as the applied load is increased so is the contact angle; nevertheless, the stand-off height becomes shorter.

**Keyword:** Surface Evolver, solder shape, package

[1] Corresponding author. E-mail: hclinh@gmail.com, Tel: +886-6-2426135.
[2] Department of Engineering Science, National Cheng Kung University.
[3] Department of Computer Application Engineering, Far East University.

## 1 Introduction

The package for electronic components has evolved from simple DIP to current complex flip chip formality. The constituents in the package are also of variety which complicates the package reliability assessment. Among the constituents, the solder bumps/balls play a crucial role as they are responsible for signal transmission, heat conduction, and energy absorption resulted from structural deformation due to thermal expansion coefficient mismatch of the various constituents. Complicating the concerns of reliability issue is the fact that solder is above half of its melting point at room temperature. It is anticipated that under the normal operating temperature the deformation kinetics is dominated by creep process. Besides, solder reliability has been reported to be package dependent. Among the factors that influence the reliability of the solder, the stand-off height and the contact angle of reflow solder balls are of interest to the present study. Previous researches devoted to the prediction of the solder shape include the work by Goldman (1969), who proposed a truncated sphere method which is purely a geometrically-based algorithm. The truncated sphere method can predicted the stand-off height of the solder ball to some accuracy. On the other hand, Heinrich (1996) employed the force-balanced approach to predict the shape of a solder ball. The force-balanced approach is capable of providing accurate prediction under the assumption that the surface of the molten solder droplet is an arc with constant curvature and the shape is formed as the arc revolves a referenced axis. Chiang (1998) applied the Surface Evolver to predict the shape of reflowed solder joints and, subsequently, analyzed stresses and strained incurred in the joints. Kaminishi (2000) use the finite element analysis program consists of the subroutines for the automatic element re-generation to simulate the fatigue crack growth in the solder joints. Chiang (2001) compared the predicative efficiency among the approaches of truncated sphere method, force-balanced method, and energy-based method. Heinrich's work was extended by Chen (2002) to the development of an approach that was applicable to both non-solder mask defined (NSMD) and solder mask defined (SMD) solder joints. Liu (2003) evaluate the effects of the solder joint shape and height on thermal fatigue lifetime with experiments. Solder joint fatigue lifetime was evaluated using accelerated temperate cycling and adhesion test. Experimental results indicated that both hourglass shape and great stand-off height could improve solder joint fatigue lifetime. Further, Chen (2005) developed a computational model using the Surface Evolver program to analyze the stability of solder bridging for area array type packaging. In his work, many factors that affect the stability of solder bridging spanning two identical circular pads were considered and the model developed was practically applicable to predict the stability of solder bridging. Cheng(2005) Use Surface Evolver to determine the geometry profile of solder joints with the modified global/local finite element modeling technique to generate the thermal-mechanical modeling of solder joints in an area array typed electronic package for characterizing the associated solder joint fatigue life under the JEDEC temperature cycling specification. Lin (2006), firstly use Surface Evolver to construct the solder based non-solder mask defined (NSMD) pad, than applied to the finite element software, ANSYS to create a double symmetric 3-D numerical model of the wafer level chip scale IC package (WLCSP) to investigate the mechanical behaviors including deformation, stress-strain relation as well as hysteresis loops for temperature cycles. The Garofalo-Arrhenius Creep Model is employed. A modified Coffin-Manson formula is also employed to estimate the fatigue life for the package. Finally, the Taguchi robust analysis is adopted for optimization analysis of UBM thicknesses and the solder geometry. Chen (2006) also extended his previous work to develop an accurate and efficient analytical geometric method to predict the geometric parameters of C4 solder joint using direct chip attach technology after a reflow process. The method was able to predict consistent results which were compared with those obtained using the Surface Evolver program, the extended Heinrich's model, and the experimental results. In present study the geometry of the solder bump is firstly estimated using free computer software, the Surface Evolver. The solder bump is then numerically constructed in a finite element model that simulates a BGA package. The influences of the upper and bottom solder pad radii, the surface tension on the balls, and the external load axially applied to the reflow solder on the standoff height and the contact angle for both solder material are then investigated accordingly.

## 2 Method for prediction

The Surface Evolver, an energy-based approach, is an interactive program for the study of liquid droplet surfaces shaped by surface tension and other energies. Liquid droplet equilibrium is achieved and the shape is determined when the energies are minimized by a gradient descent method. In the Surface Evolver, a fully 3D surface is discretized into a set of simplicial complex, that is, a union of triangles. When one applies the program, boundary conditions and energy integrals including fixed constraints, surface tension forces, droplet's volume as well as density are the inputs. The Surface Evolver is robust in analyzing a single 3-D solder bump/ball, and it has been successfully applied for predicting the final shape of the solder joint after reflow for various pad sizes, solder volumes, solder heights, and surface tensions. Details of the Surface Evolver can be referred in Brakke (2005). A brief description of the application of the Surface Evolver follows. To evaluate the shape of the solder, the restoring force in the direction of gravity is firstly determined by perturbing the upper solder pad as shown in Figure 1. When the pad is perturbed, say upward, the variational total energy associated with the solder standoff height, $H$, is expressed as

$$\delta E_t = \rho g \iint_s \left( \left( \nabla \cdot \frac{z^2}{2}\vec{k} \right) \vec{h} - \nabla \times \left( \vec{h} \times \frac{z^2}{2}\vec{k} \right) \right) d\vec{A} + T \iint_s \left( \nabla \cdot \vec{h} - \vec{n} \cdot d\vec{h} \cdot \vec{n} \right) dA - p \iint_s \vec{h} \cdot d\vec{A} \quad (1)$$

where $E_t$ is the total energy, $\rho$ is the density, $g$ is the gravitational acceleration, $\vec{k}$ is the directional unit vector along with the revolving axis of the solder ball, $\vec{n}$ is normal unit vector, $T$ is the surface tension, and $p$ is the vertical external load. In the above equation, the quantity, $\vec{h}$, expressed as

$$\vec{h} = \left[ (z_{top} - z) / (z_{top} - z_{base} - H) \right] \vec{k} \quad (2)$$

is a perturbation function, in which $z_{top}$ and $z_{base}$ are respectively the top and bottom boundary of the solders. The restoring force, $F_r$, is the derivative of the total energy with respect to the solder standoff height,

$$F_r = \frac{\partial E_t}{\partial H} = \frac{\partial E_g + \partial E_s + \partial E_f}{\partial H} \quad (3)$$

in which $E_g$ is the gravitational energy of the solder, $E_s$ is the surface tension energy, and $E_f$ is the energy due to external forces; in other words,

$$\frac{\partial E_g}{\partial H} = \rho g \iint_s \left( \left( \nabla \cdot \frac{z^2}{2}\vec{k} \right) \vec{h} - \nabla \times \left( \vec{h} \times \frac{z^2}{2}\vec{k} \right) \right) dA \quad (4)$$

$$\frac{\partial E_s}{\partial H} = T \iint_s \left( \nabla \cdot \vec{h} - \vec{n} \cdot d\vec{h} \cdot \vec{n} \right) dA \quad (5)$$

$$\frac{\partial E_f}{\partial H} = -p \iint_s \vec{h} \cdot d\vec{A} \quad (6)$$

## 3 Validation of the model

In this analysis, the shape of a reflow solder ball is modeled with the Surface Evolver. A 3D solder ball, shown in Figure 2, is created for the subsequent parametric study. Validation of the model is conducted by comparing the output with that of the Heinrich's model, a force-balanced approach. The inputs to the solder ball model include the solder volume, $V$, the radii of the upper solder pad and lower solder pad, $r_u$ and $r_l$, respectively. The upper and lower contact angles of solder surface and the pads, $\theta_u$ and $\theta_l$, respectively, and solder standoff height, $H$, are the output. The above parameters are shown in Figure 3, a schematic section plot of the solder ball.

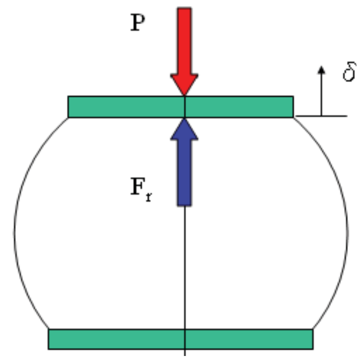

Figure 1: Schematic of the solder ball model; $p$ is the external load, $F_r$ is the restoring force, $\delta$ is the perturbed offset

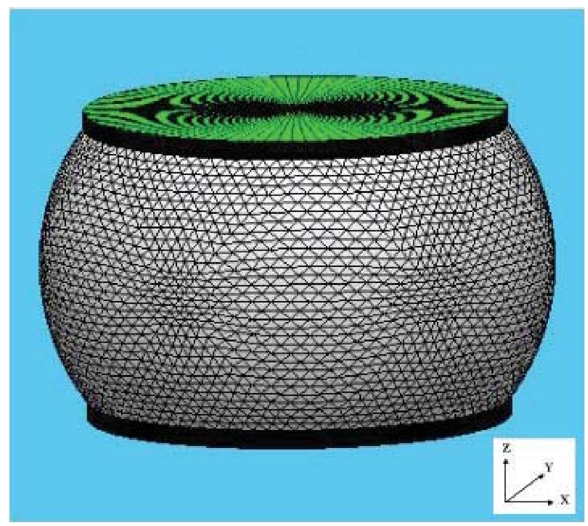

Figure 2: The 3D solder ball modeled with the Surface Evolver

### *Comparison of Surface Evolver and Heinrich models*

Three cases are employed for the comparison. In the first two cases, both the upper and lower solder pad radii are kept the same; that is, 0.1 mm for the first case and 0.3175 mm for the second case. In Case 3, the lower pad radius is greater that that of the upper one. The parameters set for the compar-

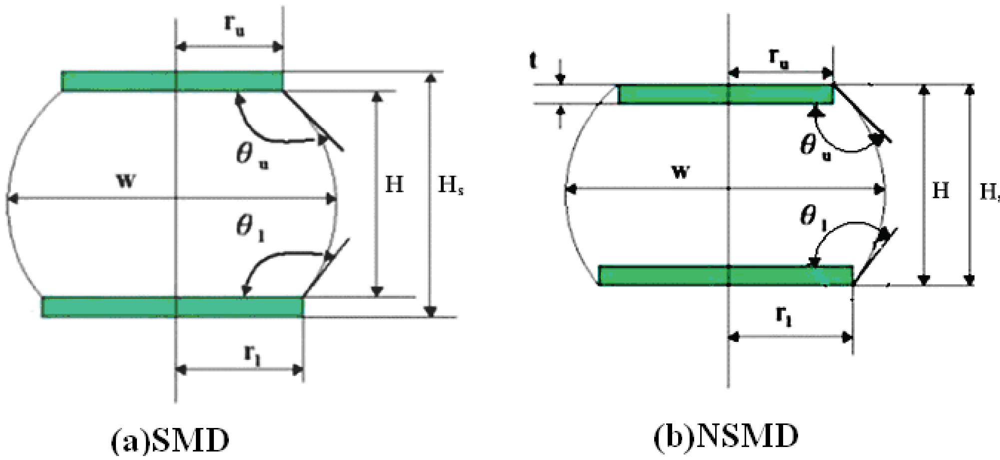


Figure 3: A section view of the solder ball and parameters

Table 1: Parameters associated with the validation for the model

| case | $r_l$ | $r_u$ | $V$ | $T$ | $p$ |
|---|---|---|---|---|---|
| 1 | 0.1 | 0.1 | 0.00314 | 40.0 | 5.5 |
| 2 | 0.3175 | 0.3175 | 0.24132 | 32.5 | 23.0 |
| | | | | | 0 |
| | | | | | -32.0 |
| 3 | 0.35 | 0.30 | 0.26 | 40.0 | 7.848 |

$^{r_l}$ radius of the lower solder pad (mm)
$^{r_u}$ radius of the lower solder pad (mm)
$^{V}$ solder volume(mm$^3$)
$^{T}$ surface tension (dyne/mm)
$^{p}$ external force (dyne)

Table 2: Comparison of solder standoff height predicted by Surface Evolver and Heinrich model

| Case | solder stand-off height by Heinrich model (mm) | solder stand-off height by Surface Evolver (mm) | error % |
|---|---|---|---|
| 1 | 0.0848 | 0.0852 | +0.47 |
| 2 | 0.453 | 0.469 | +3.53 |
| | 0.524 | 0.525 | +0.19 |
| | 0.753 | 0.745 | -1.06 |
| 3 | 0.510 | 0.520 | +1.96 |

ison are listed in Table 1. It is also noted that in Case 2, three various external lords are selected for further comparison. Table 2 presents the results of solder heights predicted by the two approaches. It can be seen that in most cases (4 out of 5), Heinrich model predicts shorter solder heights than the Surface Evolver does. However, as both models predict quite well and close to one another (with 4%), it may considered the model adopted in this study for evaluating the BGA solder ball shape is adequate.

Comparison of the solder shape in terms of solder height and contact angle predicted by the Surface Evolver and Heinrich Model is carried out on the following basis. The solder volume is 0.230 mm$^3$, the reflow temperature is 380$^o$C corresponding to a surface tension of 481 dyne/cm, and the external applied load is 7.85 dynes. Figure 4 shows the predicted solder heights by the two approaches. It is seen that both approaches predict that the solder height decreases as the pad radii (both upper and lower ones) increase. It is also interesting to see that at smaller pad radius, below 0.25 mm, there is apparent deviation on solder height prediction. Figure 5 presents the contact angles predicted by the tow approaches. It is seen that as pad radii becomes greater, the contact angle becomes smaller. A further observation discloses that the contact angle predicted by Heinrich Model is greater that by the Surface Evolver. The deviation on prediction is with 5% as the pad radii kept larger than 0.20 mm.

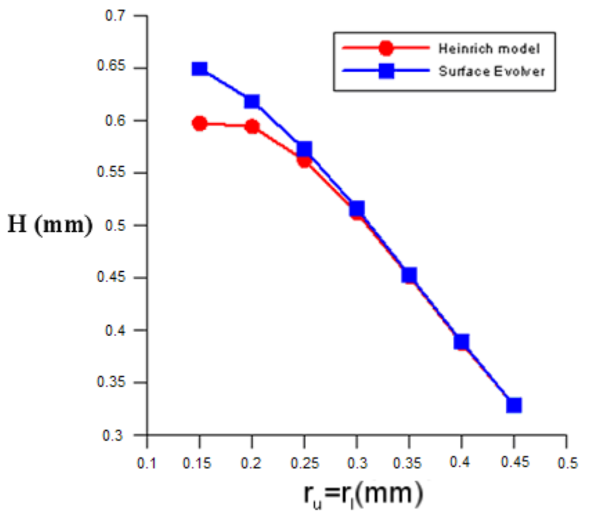


Figure 4: Comparison of solder heights predicted by Surface Evolver and Heinrich model

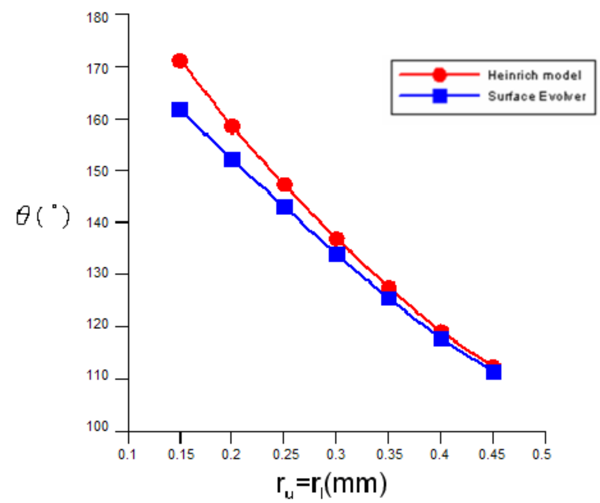


Figure 5: Comparison of contact angle predicted by the Surface Evolver and Heinrich model

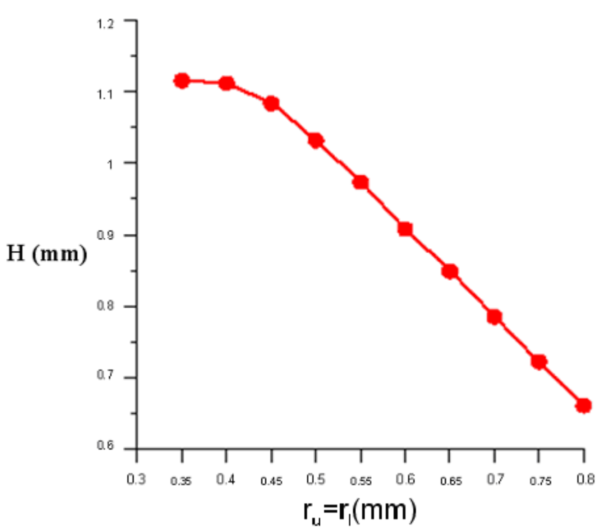


Figure 6: Effects of solder pad radii on the solder height. ($r_u = r_l$)

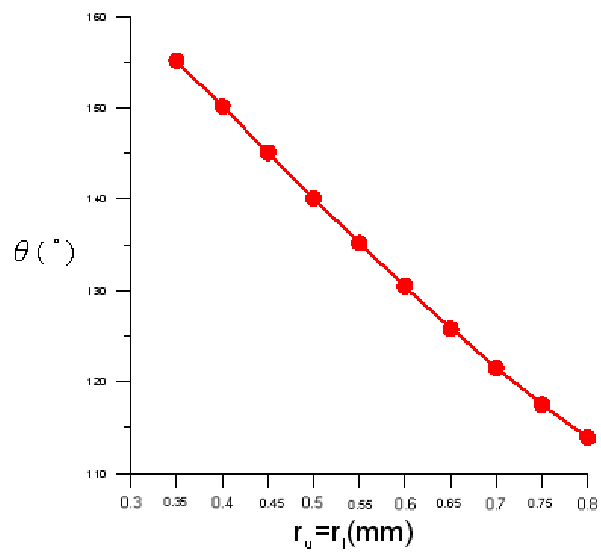


Figure 7: Effects of solder pad radii on the solder contact angle. ($r_u = r_l$, hence $\theta_u = \theta_l$)

## 4 Results and discussion

### *Effects of solder pad radii on solder shape*

To study the effects of pad radius, it is necessary to assume the volume of the solder to be constant. It is also assume both the upper pad and the lower pad radii be the same during the course of the study. The solder volume is 1.5 mm$^3$ and has a density of 8.42 g/cm$^3$, the reflow temperature is 380°C which corresponds to a surface tension of 481 dyne/cm, and the applied external load is 10 dynes. Shown in Figure 6 are the effects of pad radius on the solder height. Figure 6 indicates a down trend of solder height with the augment of pad radius. However, it is also noted the height change insignificantly as the pad radius is less than 0.4 mm. The effects of pad radius on contact angle are shown in Figure 7. There is a

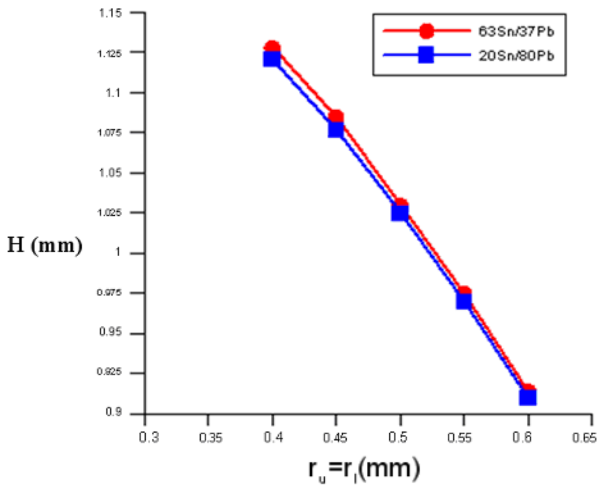


Figure 8: Comparison of the solder height for solders Sn37Pb and Sn80Pb

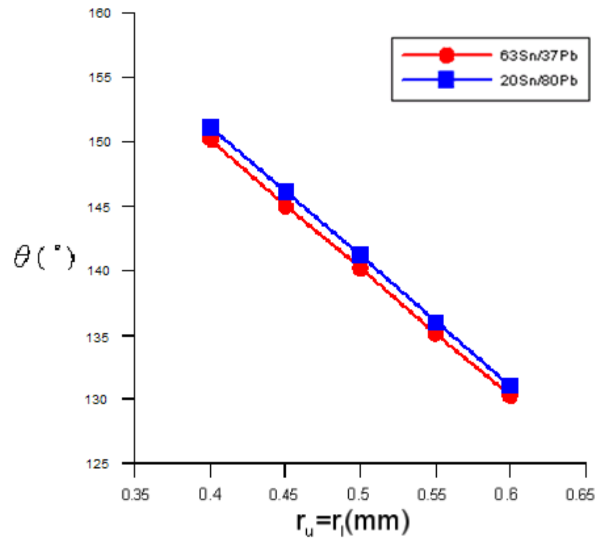


Figure 9: Comparison of the contact angles for solders Sn37Pb and Sn80Pb

similar trend of the effects of pad radius on the contact angle; that is, smaller pad radius tends to increase the contact angle of the solder shape.

***Effects of solder material on solder shape***

Two different solders are considered for this investigation, viz., Sn37Pb and Sn80Pb. The material properties of these solders are referred in Manko (1992). The solder volume is 1.5 $mm^3$ and the external load is 10 dynes for both solders. Both solders are subjected to a reflow temperature of 280°C corresponding to a surface tension of 490 dyne/cm for Sn37Pb and 467 dyne/cm for Sn80Pb. The densities are 8.42 $g/cm^3$ and 10.27 $g/cm^3$ for Sn37Pb and Sn80Pb, respectively. It is assumed that both solder pad radii are kept the same. The results of the effects on solder height and on contact angle are shown in Figures 8 and 9, respectively. These figures demonstrate that both the solder height and the contact angle decrease as the pad radius increases.

***Effects of surface tension on solder shape***

The surface tension is related to the reflow temperature in the manufacturing process. To investigate the effects of surface tension on the shape of the Sn37Pb solder, it is assumed that the solder volume is 2.0 $mm^3$, both solder pad radii are 0.6 mm, the solder density at 8.42 $g/cm^3$, and the solder is subjected to an external load of 15 dyne. It can be seen in Figure 10 that the solder height increases with the surface tension. However, the height tends to be saturated beyond a surface tension of 600 dyne/mm. Shown in Figure 11 is the effects the surface tension on the contact angles. As both upper and lower solder pad radii are kept the same, the contact angle, either upper or lower one, decreases as the surface tension increases.

***Effects of external load on solder shape***

In this part of the study, the parameters associated with the Sn37Pb solders are set as follows. The solder volume is set at 2.0 $mm^3$, both solder pad radii at 0.6 mm, the surface tension at 481 dyne/cm, the reflow temperature at 380°C, and the solder density at 8.42 $g/cm^3$. The applied external load is considered positive if the perturbed offset is downward, and negative upward. The solder standoff height and the contact angles are of interest. Shown in Figure12 is the effect of the external load on the solder height and in Figure 13 the effect on the contact angles. It can be seen that at constant solder volume, the solder height decreases with the downward external load. Note that in Figure 12 the increasing value on abscissa

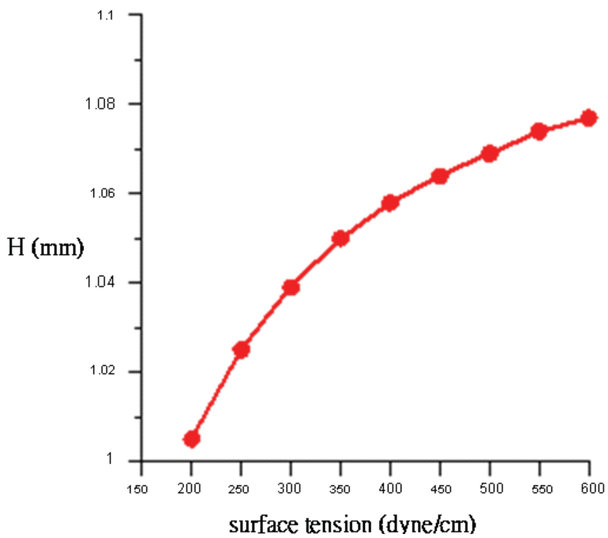


Figure 10: Effects of surface tension on solder height

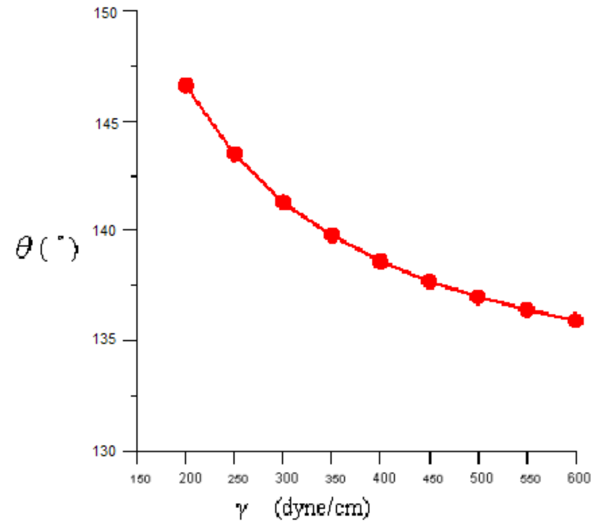


Figure 11: Effects of surface tension on contact angle

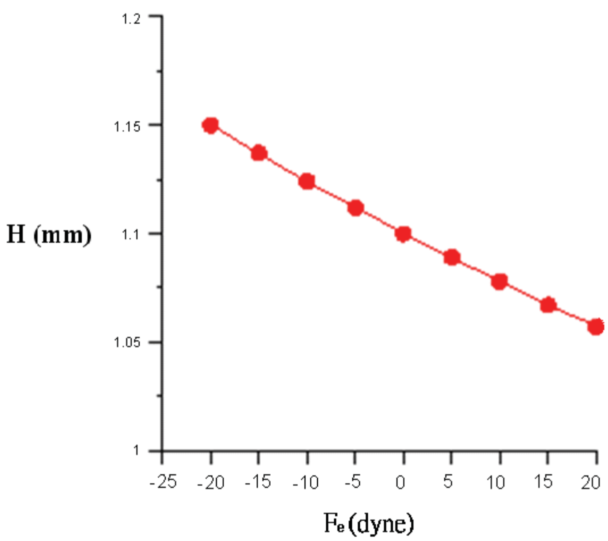


Figure 12: The effects of external load on solder height

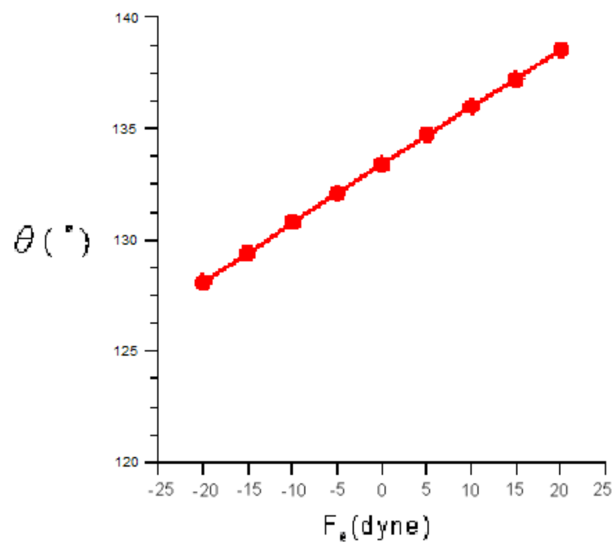


Figure 13: The effects of external load on solder contact angle

represents increasing downward external load. On the other hand, the contact angle decreases as the downward external load increases.

## 5 Conclusion

A parametric study is presented in this study. The surface Evolver is employed to create a numerical model of a BGA solder ball for the parametric study. Some parameters are selected to investigate their effects on the solder height as well as the contact angle. It may conclude that the Surface Evolver can predict the solder shape as well as the Heinrich model. At a constant volume of the solder ball, both the solder height and the contact angle reduce when the pad radii (upper and lower ones) increase simultaneously. The study of the effects of solder material on solder shape reveals that, at constant solder volume, both of the solder height and contact angle decrease as the pad radii becomes large. However, due to a greater density of Sn80Pb, the solder height and the contact angle for Sn80Pb solder are less than those of Sn37Pb. The surface tension, at constant solder volume, had a positive influence on solder height. An inverse trend is found of the effects of the surface tension of the contact angle. Finally, a downward external load tends to shorten the height of the solder ball and augment the contact angle.

## Reference

**Brakke, K. A.** (2005): Surface Evolver Manual, version 2.26, Selinsgrove, PA.

**Chiang K.N.; Chen W.L.** (1998): Electronic Packaging Reflow Shape Prediction for The Solder Mask Defined Ball Grid Array, *ASME Transaction, Journal of Electronic Packaging*, Vol. 120, pp. 175-178.

**Chiang K.N.; Yuan C.A.** (2001): An Overview of Solder Bump Shape Prediction Algorithms with Validations, *IEEE Transactions on Advanced Packaging*, Vol.24, No.2, pp.158-162.

**Chen W.H.; Chiang K.N.; Lin S.R.** (2002): Prediction of Liquid Formation for Solder and Non-Solder Mask Defined Array Packages, *ASME Journal of Electronic Packaging*, Vol. 124, pp.37-44.

**Chen, W.H.; Lin, S.L.; Chiang, K.N.** (2005): Stability of Solder Bridging for Area Array Type Packaging, *CMC: Computers, Materials and Continua*, Vol. 2, No.3, pp. 151-162.

**Chen, W.H.; Lin, S.L.; Chiang, K.N.** (2006): Prediction of Liquid Formation for C4 Type Solder Joints in Flip Chip Technology, *ASME Journal of Electronic Packaging*, Vol. 128, No. 4, pp. 331-339.

**Cheng, H. C.; YU, C. Y.; Chen, W.H.** (2005): An Effective Thermal-mechanical Modeling Methodology for Large-scale Area Array Typed Packages, *CMES: Computer Modeling in Engineering & Sciences*, Vol. 7, No. 1, pp. 1-18.

**Goldmann, L.S.** (1969): Geometric Optimization of Controlled Collapse Interconnection , *IBM Journal of Research and Development*, vol. 120, pp. 175-178.

**Heinrich , S.M.; Schaefer, M.; Schroeder, S.A.; Lee, P. S.** (1996): Prediction of Solder Joint Geometry in Array-Type Interconnects, *ASME J. Elec. Pack.*, Vol. 118, No. 3, pp. 114-121.

**Kaminishi, K.; Iino, M.; Bessho, H.; Taneda, M.** (2000): Numerical Simulation of Fatigue Crack Growth in Microelectronics Solder Joints, *CMES: Computer Modeling in Engineering & Sciences*, Vol. 1, No. 1, pp. 107-110.

**Lin, H. C.; Kung, C.; Chen, R. S.; Liang, G. T.** (2006): An Optimization Analysis of UBM Thicknesses and Solder Geometry on A Wafer Level Chip Scale Package Using Robust Methods, *CMC: Computers, Materials and Continua*, Vol. 3, No. 2, pp. 55-64.

**Liu, X.; Lu, G.** (2003): Effects of Solder Joint Shape and Height on Thermal Fatigue Lifetime, *IEEE Transactions on Components and Packaging Technologies*, Vol. 26, No. 2, pp. 455-465.

**Manko, H.H.** (1992): Solders and soldering: materials, design, production, and analysis for reliable bonding, McGraw-Hill, New York.